E-ISSN 2586-9027
Homepage : *https://tci-thaijo.org/index.php/SciTechAsia* Science & Technology Asia
Vol.30 No.2 April - June 2025 Page: [204-226]
Original research article

Data Preprocessing Enhancement for Artificial Neural Networks in Predicting Mechanical Properties of Dual-Phase Steel

Anan Butrat[1], Patiparn Ninpetch[2,*]

[1] *Department of Industrial Management Engineering, Faculty of Industrial Technology, Valaya Alongkorn Rajabhat University under the Royal Patronage, Pathum Thani 13180, Thailand*
[2] *Department of Industrial Engineering, Faculty of Engineering, Rajamangala University of Technology Thanyaburi, Pathum Thani 12120, Thailand*

Received 28 November 2024; Received in revised form 28 April 2025
Accepted 19 May 2025; Available online 18 June 2025

ABSTRACT

The mechanical properties of Dual-phase (DP) steel, including toughness and hardness, are influenced by the intercritical annealing process parameters, such as temperature, holding time, and cooling rate. Traditional regression models have limitations in accurately predicting these nonlinear relationships. This study addresses the challenge by introducing a data preprocessing method, the Regression-Based Data Preprocessing (RBDP) method, aimed at improving the accuracy of Artificial Neural Network (ANN) models in predicting toughness and hardness of DP steel. The RBDP method enhances the training dataset by generating synthetic data through regression analysis, allowing for more robust ANN performance. The mechanical properties of nine DP steel specimens were analyzed using RBDP combined with ANN models and compared with predictions from pure ANN models and traditional regression approaches. For hardness prediction, the PRH + ANN model emerged as the most accurate, achieving the lowest average error of 0.72%, performing particularly well for specimens 1, 3, 4, and 9. For toughness prediction, the PRT + ANN model was the most effective, delivering the lowest prediction errors across most specimens, with particularly low errors for specimens 1, 4, 5, 7, 8, and 9. Both PRH + ANN and PRT + ANN models outperformed traditional regression approaches and standalone ANN models. These findings demonstrate that the proposed RBDP method significantly improves the accuracy of ANN models for predicting the mechanical properties of DP steel. This study highlights the potential to enhance predictive modelling in materials science.

Keywords: Data Preprocessing Enhancement; Dual-phase steel; Artificial neural networks; Mechanical properties prediction; Machine learning

***Corresponding author:** Patiparn.n@en.rmutt.ac.th **doi:** 10.14456/scitechasia.2025.36

1. Introduction

Dual-phase (DP) steel is an advanced high-strength steel (AHSS) developed through intercritical annealing to obtain a dual-phase structure consisting of ferrite and martensite [1]. The intercritical annealing process for DP steel production involves heating the steel to temperatures between Ac1 and Ac3 (typically 720°C to 900°C), resulting in a ferrite-austenite $(\alpha + \gamma)$ structure, followed by rapid cooling (quenching) in water or oil [2, 3]. During quenching, the austenite phase transforms into martensite, while the ferrite phase remains unchanged [4]. The combination of hard martensite islands distributed in a soft ferrite matrix imparts DP steel with excellent ductility, high hardness, high tensile strength, and toughness [5]. These properties have led to widespread use in the automotive industry, particularly for parts requiring a balance of strength, ductility, and formability, such as structural elements [6, 7]. To meet specific application requirements in DP steel, controlling intercritical annealing parameters (temperature, holding time, and cooling rate) is crucial. Singh et al. [8] reported that intercritical annealing temperature and holding time significantly affect the martensite volume fraction in DP steel. They found that increasing these parameters leads to higher hardness and toughness [8]. Consequently, investigating the effects of intercritical annealing process parameters is vital for developing DP steel with desirable mechanical properties. The impact of intercritical annealing process parameters is nonlinear and complex, making it challenging to explain the relationships between multiple parameters using traditional regression models such as linear and multiple regression [9]. Moreover, the intercritical annealing process for DP steel often requires extrapolation because evolving application demands—like new automotive components—necessitate process parameters (e.g., temperature, holding time) beyond previously studied conditions. Due to the complex, nonlinear interactions of these parameters, traditional datasets may not cover all scenarios. As a result, machine learning models trained on limited data struggle to predict mechanical properties outside the training range, leading to reduced accuracy. Extrapolation poses a major challenge as models make assumptions about unseen regions. To address this, strategies like dataset expansion, synthetic data generation, and regression-based preprocessing methods can enhance prediction reliability and performance.

In recent years, machine learning (ML) models have been developed and applied to predict the mechanical properties of metal alloys [10, 11]. ML models are powerful statistical analysis techniques capable of capturing internal linear and nonlinear relationships using empirical data [12]. Several studies have focused on developing and implementing ML models to predict material mechanical properties [13, 14]. Agrawal and Choudhary [15] introduced various machine learning methods applied to materials science, highlighting challenges in data management within the field, and emphasizing the potential of materials informatics to significantly reduce time and costs in materials development. Liu et al. [16] provided a comprehensive review of machine learning applications in materials science, particularly for materials discovery and design. Artificial Neural Networks (ANNs) are a prominent ML technique for defining nonlinear and complex relationships between multiple parameters without being constrained by specific regression models. Additionally, Jha et al. [17] presented algorithms for optimizing the chemical composition of hard magnetic alloys and Agarwal et al. [18] investigated void growth in 6061-aluminum alloy under triaxial stress conditions have successfully applied ANNs in materials science. However, preliminary studies using ANNs to predict mechanical properties have shown that they may not always precisely match experimental results for hardness and toughness.

In the context of predicting the mechanical properties of dual-phase (DP) steel using machine learning (ML), data preprocessing is an essential step that significantly impacts model performance. It involves preparing raw data for analysis through tasks such as cleaning, normalization, feature selection, and encoding, which help improve data quality, reduce bias, and increase model accuracy. However, traditional pre-processing methods often struggle when models are required to predict values outside the range of the training data, a challenge known as extrapolation. To address this limitation, the proposed Regression-Based Data Preprocessing (RBDP) method introduces regression modeling as a key component in the preprocessing phase. This approach uncovers and reinforces the underlying relationships between the intercritical annealing parameters and the mechanical properties of DP steel. By generating synthetic data based on regression trends, RBDP expands the training dataset and provides Artificial Neural Networks (ANNs) with a more diverse and pattern-rich input space. As a result, RBDP not only improves the model's generalization ability but also enhances its capacity to make more accurate predictions for out-of-range data, effectively addressing extrapolation challenges.

This study introduces the Regression-Based Data Preprocessing (RBDP) method to enhance the predictive performance of Artificial Neural Networks (ANNs) in extrapolating the mechanical properties of dual-phase (DP) steel, such as toughness and hardness, beyond the training dataset range. RBDP strengthens regression-based relationships between intercritical annealing parameters and mechanical properties, enabling the model to generalize and make accurate predictions for out-of-range data. By generating synthetic data based on regression trends and expanding the dataset, RBDP provides a more diverse training set, improving the model's generalization ability.

This method addresses the limitations of traditional data preprocessing for extrapolation tasks and will be evaluated against conventional ANN and regression models to demonstrate its effectiveness in materials science applications.

2. Methods

This study proposes a methodology for Regression-Based Data Preprocessing (RBDP) method as shown in Fig. 1. As the first step, data collection (mechanical property experiments) is divided into two categories: in-learning-range data and out-learning-range data. For in-learning-range data, multiple regression models were first identified, including Linear, Exponential, Logarithmic, and Polynomial models to ensure a comprehensive evaluation. Information required for synthetic data generation was then determined, specifying the maximum range, minimum range, and increment step. Using these parameters, synthetic data was generated and subsequently duplicated. The data was then split appropriately for training and validation purposes. Feature selection was conducted to identify the most relevant inputs, followed by model selection based on the chosen regression

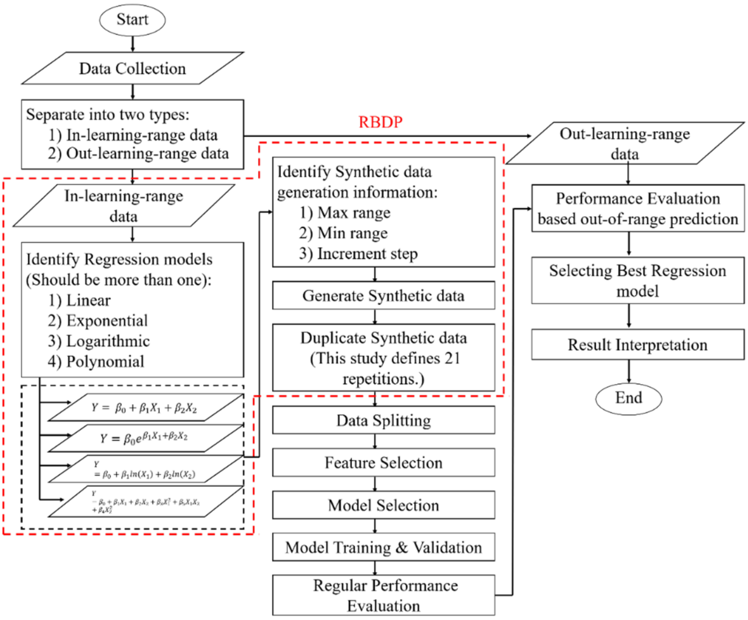

Fig. 1. The method of RBDP.

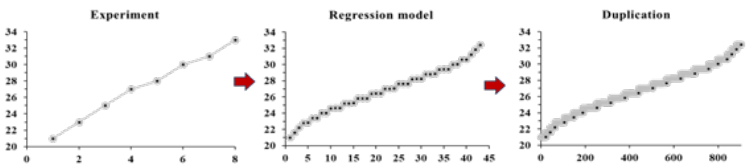

Fig. 2. The step of hardness data before and after RBDP.

types. Model training and validation were carried out systematically, with regular performance evaluations performed throughout the process to monitor model behavior. For out-learning-range data, model performance was evaluated based on the models' ability to predict beyond the original training range. The best-performing regression model was selected based on overall evaluation metrics. Finally, the results were interpreted to provide insights into model behavior and predictive capabilities (see Fig. 2).

2.1 Data of mechanical properties of DP steel

The experimental data for this study, sourced from Singh et al. [19], focused on medium carbon steel (0.46 wt% C) subjected to intercritical annealing. Specimens (10 mm thick) were annealed at temperatures (Temp) of 760°C, 800°C, and 840°C for 2, 4, and 6 minutes of holding time (HT), followed by water quenching to achieve a dual-phase microstructure. Mechanical properties, including hardness (Rockwell scale C) and toughness (Charpy impact test), were measured for each specimen. Table 1 presents the mechanical properties of the DP steel specimens [19]. This experiment is applied to be the case study of the RBDP method. In the initial preprocessing stage, the data was partitioned into two categories including the source dataset that comprises the first 8 specimens, and the

Table 1. Mechanical properties of the DP steel specimens [19].

Specimens	Temp °C	HT (min)	Toughness (J)	Hardness (HRC)	In-learning-range data	Testing data	Prediction data
1	760	2	67	21			
2	760	4	71	23			
3	760	6	73	25			
4	800	2	78	27			
5	800	4	80	28	Yes	Yes	Yes
6	800	6	82	30			
7	840	2	84	31			
8	840	4	86	33			
9	840	6	87	34	No	No	

target dataset that comprises all 9 specimens that need to be predicted after the prediction model is completed. Notably, specimen 9 (840°C, 6 minutes, yielding 87 J toughness and 34 HRC hardness) was exclusively allocated to the Predicting Dataset. This strategic data separation ensures that the Artificial Neural Network (ANN) model remains unaware of the specific relationship between the 840°C annealing temperature and 6-minute holding time during the training phase, allowing for an unbiased assessment of the model's predictive capabilities for this heat treatment condition.

2.2 Regression models

Regression models including linear, exponential, logarithmic, and polynomial are compared to identify the best fit for describing the relationship between intercritical annealing parameters and the mechanical properties of dual-phase (DP) steel. The first step of RBDP was to find the regression of the first 8 specimens by using the four types of the regression models, including Linear, Exponential, Logarithmic and Polynomial.

2.2.1 Linear regression

Linear regression is a statistical method used to model the relationship between the target and one or more features. The goal is to fit a straight line that best represents the relationship between the variables. The Relationship Model with two features, including Temp and HT, could be:

$$Y = \beta_0 + \beta_1 X_1 + \beta_2 X_2, \qquad (2.1)$$

where β_0 is the intercept, and β_1, β_2 are the coefficients for Temperature and Holding Time, respectively. The X_1 is Temperature, the X_2 is Holding Time and Y is Toughness. or Hardness. The Linear Regression for toughness (LiRT) is shown in Eq. (2.2) and the Linear Regression for Hardness (LiRH) is shown in Eq. (2.3).

$$LiRT = -88.60 + 0.20 \times Temp + 1.31 \times HT, \qquad (2.2)$$

$$LiRH = -75.20 + 0.12 \times Temp + 0.91 \times HT. \qquad (2.3)$$

2.2.2 Exponential regression

Exponential regression is a type of regression analysis used to model situations where the growth or decay of the dependent variable follows an exponential pattern. It is useful when data shows a consistent rate of change (either increase or decrease) proportional to the value of the dependent variable itself. The Relationship Model with two features, including Temp and HT, could be:

$$Y = \beta_0 e^{_1 X_1 + _2 X_2}. \tag{2.4}$$

The Exponential Regression for toughness (ERT) is shown in Eq. (2.5) and The Exponential Regression for Hardness (ERH) is shown in Eq. (2.6).

$$ERT = 8.84e^{(0.002645 \times Temp + 0.017695 \times HT)}, \tag{2.5}$$

$$ERH = 0.58e^{(0.004652 \times Temp + 0.035888 \times HT)}. \tag{2.6}$$

2.2.3 Logarithmic regression

Logarithmic regression is a type of regression analysis used to model situations where the rate of change of the dependent variable decreases as the independent variable increases. It is typically applied when the relationship between the independent and dependent variables follows a logarithmic pattern, meaning the change in the dependent variable slows down as the independent variable grows larger. The Relationship Model with two features, including Temp and HT, could be:

$$Y = \beta_0 + \beta_1 \ln(X_1) + \beta_2 \ln(X_2). \tag{2.7}$$

The Logarithmic Regression for toughness (LoRT) is shown in Eq. (2.8) and The Logarithmic Regression for Hardness (LoRH) is shown in Eq. (2.9).

$$LoRT = -999.99 + 160.548453 \times \ln(Temp) + 4.511266 \times \ln(HT), \tag{2.8}$$

$$LoRH = -632.54 + 98.237081 \times \ln(Temp) + 3.096521 \times \ln(HT). \tag{2.9}$$

2.2.4 Polynomial regression

Polynomial regression is a type of regression analysis in which the relationship between the independent variable and the dependent variable is modeled as an n-th degree polynomial. This method is used when the data does not follow a linear relationship and instead exhibits curvature. The Relationship Model with two features, including Temp and HT, could be:

$$Y = \beta_0 + \beta_1 X_1 + \beta_2 X_2 + \beta_3 X_1^2 + \beta_4 X_1 X_2 + \beta_5 X_2^2. \tag{2.10}$$

The polynomial Regression for toughness (PRT) and Hardness (PRH) are shown in Eqs. (2.11)-(2.12).

$$PRT = -940.86 + 2.304167 \times Temp + 10.761905 \times HT - 0.001295 \times Temp^2 - 0.010714 \times (Temp \times HT) - 0.142857 \times HT^2, \tag{2.11}$$

$$PRH = -250.14 + 0.558333 \times Temp + 2.154762 \times HT - 0.000268 \times Temp^2 - 0.001786 \times (Temp \times HT) + 0.017857 \times HT2. \tag{2.12}$$

Among various approaches to synthetic data generation, methods based on regression models have gained significant attention due to their ability to capture complex relationships between variables and generate realistic data points [21]. These techniques leverage the predictive power of regression models to create new, synthetic instances that follow the same patterns and distributions as the original data. However, mechanical properties such as toughness and hardness are not clearly defined

Table 2. Synthetic data generation information.

Features	Max	Min	Increment step	Total amount
Temperature (°C)	840	760	5	43
Holding time (min)	2	6	2	

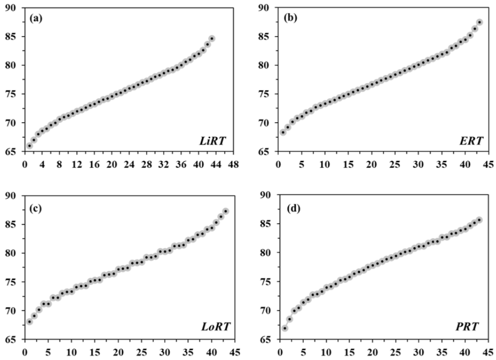

Fig. 3. Toughness regression: (a) LiRT, (b) ERT, (c) LoRT, (d) PRT.

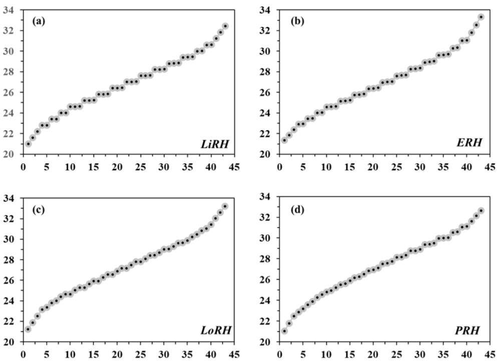

Fig. 4. Hardness regression: (a) LiRH, (b) ERH, (c) LoRH, (d) PRH.

as regression models. Therefore, synthetic data in this study was generated based on the equations that were found in section 2.2 and followed by the range and increment step in Table 2. Within ranging and increment steps, 43 specimens of synthetic data include the dataset of toughness as shown in Fig. 3 and the dataset of hardness as exhibited in Fig. 4.

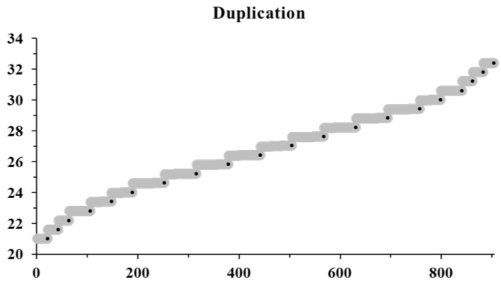

Fig. 5. Example of dataset after data duplication.

2.3 Data duplication

Data duplication in Artificial Neural Networks (ANNs) involves replicating data points to address various challenges such as class imbalance and dataset size limitations. By duplicating underrepresented data, this technique helps balance the dataset, reducing model bias and improving fairness in predictions. It can also enhance model robustness by providing more diverse training examples, which stabilizes training and can indirectly reduce overfitting.

Data duplication is a form of data augmentation that contributes to better generalization and more reliable model performance. For instance, Chawla et al. [22] discussed its use in synthetic minority oversampling [22], while Shorten and Khoshgoftaar et al. [23] highlighted its role in improving image data for deep learning models [23]. In this study, the dataset of each regression model is duplicated to increase them from 43 specimens to 903 specimens, as shown in Fig. 5

2.4 Cross-validation analysis

The purpose of performing cross-validation analysis on the expanded dataset, which was generated by duplicating 43 original records (after generating synthetic data using each regression model) to create a total of 903 samples, is to assess the robustness, stability, and generalization abil-

Table 3. Cross validation for toughness prediction.

Toughness		Linear		Exponential		Logarithmic		Polynomial	
Dataset	Fold	MSE	R^2 Score	MSE	R^2 Score	MSE	R^2 Score	MSE	R^2 Score
Cross-Validation	Fold 1	0.0000	1.0000	0.0272	0.9989	0.0853	0.9966	0.4818	0.981
	Fold 2	0.0000	1.0000	0.0289	0.9989	0.0998	0.9961	0.5181	0.9792
	Fold 3	0.0000	1.0000	0.0226	0.9989	0.1139	0.9943	0.466	0.9763
	Fold 4	0.0000	1.0000	0.0243	0.9987	0.0816	0.9955	0.4432	0.9775
	Fold 5	0.0000	1.0000	0.0229	0.999	0.1009	0.9957	0.4619	0.9806
	Avg.	0.0000	1.0000	0.0252	0.9989	0.0963	0.9957	0.4742	0.9789
	Test Set	0	0.0000	1.0000	0.9989	0.101	0.9952	0.4386	0.9787

ity of regression models despite the presence of repeated data. Since duplication increases the risk of overfitting, especially if identical samples appear in both training and validation sets, the analysis carefully applies grouped cross-validation techniques to ensure that all duplicates of each original sample are kept within the same fold. This approach helps to avoid data leakage and provides a more realistic evaluation of model performance. Ultimately, this validation process supports model selection by ensuring that high accuracy is not a result of memorizing repeated data but reflects genuine predictive ability.

The regression results for predicting Toughness using four models—Linear, Exponential, Logarithmic, and Polynomial—are summarized across five cross-validation folds and the test set. The Linear model consistently achieved perfect performance with an MSE of 0.0000 and R^2 of 1.0000 across all folds and the test set, indicating an exact fit. The Exponential model showed strong performance with an average cross-validation MSE of 0.0252 and R^2 of 0.9989, and a test set MSE of 0.1010 with R^2 of 0.9952. The Logarithmic model had higher error, with average cross-validation MSE of 0.0963 and R^2 of 0.9957, and a test set MSE of 0.4386 and R^2 of 0.9787. The Polynomial model showed the weakest performance among the four, with the highest average cross-validation MSE of 0.4742 and lowest R^2 of 0.9789, while the test set results reported MSE 0.4386 and R^2 0.9787. These results suggest that the Linear model is most suitable for this dataset, while the Polynomial model, despite its complexity, offers comparatively poorer generalization. Table 3 lists cross validation for toughness prediction.

Table 4 shows cross validation for hardness prediction. The regression analysis for predicting Hardness was conducted using four models—Linear, Exponential, Logarithmic, and Polynomial—across five cross-validation folds and a test set. The Linear model achieved perfect performance with an MSE of 0.0000 and R^2 of 1.0000 across all folds and the test set, suggesting an exact fit to the data. The Exponential model showed solid performance with an average cross-validation MSE of 0.0314 and R^2 of 0.9964, and test set MSE of 0.0276 with R^2 of 0.9965. The Logarithmic model performed slightly worse, with an average cross-validation MSE of 0.0451 and R^2 of 0.9947, and test set MSE of 0.0471 and R^2 of 0.9941. The Polynomial model demonstrated strong performance with an average MSE of 0.0241 and R^2 of 0.9971, and a test set MSE of 0.0198 with R^2 of 0.9974, outperforming both Exponential and Logarithmic models. Overall, while the Linear model appears to fit perfectly, the Polynomial model offers the most robust generalization among the non-

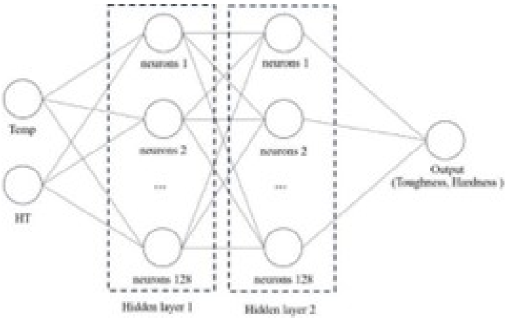

Fig. 6. ANN model structure for predicting Hardness and Toughness.

linear models.

2.5 Artificial neural networks

Applying Artificial Neural Networks (ANNs) for prediction involves data preprocessing, network design, and model training. This specific ANN model is configured for a regression task with two input features. It uses two hidden layers (128 neurons each) with ReLU activation, Adam optimization, and MSE loss function. The model was trained for 1000 epochs with a batch size of 10 and a validation split of 0.2. The data was split 80/20 for training and testing, with a random state of 42. This setup balances simplicity and effectiveness for predicting continuous outcomes based on two variables of x data including Temperature and Holding time. Regular updates and retraining were recommended to maintain model accuracy. At the end, the model provided toughness or hardness based on the y data that is the output for training and testing. Fig. 6 displays ANN model structure.

2.6 Prediction uncertainty analysis

Prediction uncertainty analysis was conducted by comparing the difference between the predicted and observed means (△Mean) and the difference between their standard deviations (△SD). △Mean measures how closely the model's central tendency aligns with the actual data, while △SD assesses how well the model captures the variability of the observed values. Smaller differences in both metrics indicate lower prediction uncertainty, reflecting higher model accuracy and reliability. This approach provides a straightforward and interpretable assessment of uncertainty in the model's predictions.

2.7 Local interpretable model-agnostic explanations contribution analysis (LIME)

The Local Interpretable Model-Agnostic Explanations (LIME) Contribution Analysis was used to interpret the model's predictions by approximating the complex model locally with a simple, interpretable model. By generating perturbed samples around each instance and analyzing the resulting predictions, LIME estimates the contribution of each input feature to the final output. Positive and negative contributions indicate how features respectively increase or decrease the prediction. This analysis provides clear insights into feature importance for individual predictions, enhancing model transparency and trust.

3. Results

3.1 Toughness prediction

The comparison of toughness prediction results for Specimen 9, as illustrated in Table 5, provides valuable insights into the effectiveness of various processes and RBDP methods. Based on experimental data from Singh et al. [19], with a temperature of 840°C and a holding time of 6 minutes, the target toughness value is 87. The results show that PRT is consistently the most accurate model for predicting values close to this target. While

Table 4. Cross validation for toughness prediction.

Toughness		Linear		Exponential		Logarithmic		Polynomial	
Dataset	Fold	MSE	R^2 Score	MSE	R^2 Score	MSE	R^2 Score	MSE	R^2 Score
Cross-Validation	Fold 1	0.0000	1.0000	0.0342	0.9965	0.0400	0.9959	0.0254	0.9973
	Fold 2	0.0000	1.0000	0.0364	0.9963	0.0468	0.9953	0.0267	0.9972
	Fold 3	0.0000	1.0000	0.0282	0.9964	0.0531	0.9929	0.0216	0.9971
	Fold 4	0.0000	1.0000	0.0299	0.9957	0.0384	0.9945	0.0246	0.9966
	Fold 5	0.0000	1.0000	0.0285	0.9969	0.0471	0.9948	0.0223	0.9975
	Avg.	0.0000	1.0000	0.0314	0.9964	0.0451	0.9947	0.0241	0.9971
	Test Set	0.0000	1.0000	0.0276	0.9965	0.0471	0.9941	0.0198	0.9974

Table 5. Comparison on toughness prediction results from each method.

Exp.		Pure data + Duplication +ANN	RBDP only				RBDP+ANN			
			LiRT	ERT	LoRT	PRT	LiRT	ERT	LoRT	PRT
S9	87	88.86	87.26	89.13	90.67	86.32	87.15	90.18	90.76	87.42
Diff	-	2.14%	0.30%	2.45%	4.22%	-0.78%	0.17%	3.66%	4.32%	0.48%

Pure Data + Duplication + ANN increases the prediction to 88.86, a range of difference of +2.14%, it does not achieve optimal accuracy. Among the individual regression models from RBDP, LiRT yields the closest prediction at 87.26 (0.30%). PRT also approximates the target with a prediction of 86.32 (-0.78%) but is less precise than LiRT. When using combined ANN approaches, LiRT and PRT again provide nearer results at 87.15 (0.17%) and 87.42 (0.48%), respectively, demonstrating its reliability for aligning predictions with the target value. Overall, LiRT + ANN proves to be the most effective model for achieving predictions that closely match the experimental target value of 87 as shown in Table 5.

However, as shown in Table 6, the prediction error results for toughness from different regression models from RBDP (LiRT, ERT, LoRT, PRT) across the target dataset including nine specimens (S1-S9). Across the nine specimens, PRT consistently delivers the lowest prediction errors, making it the most accurate model overall. It performs best in most cases, with particularly low errors for Specimens 1, 4, 5, 7, 8, and 9. ERT occasionally outperforms others, as seen in Specimens 2 and 6, but generally shows higher errors than PRT. LoRT performs well in certain cases, like Specimen 3, but is less reliable overall.

Table 6. Comparison of toughness prediction error results from regression.

Specimens	LiRT	ERT	LoRT	PRT
S1	0.81%	2.06\%	2.19%	0.09%
S2	2.73%	0.38%	0.35%	0.75%
S3	2.3%	0.04%	0.64%	0.07%
S4	5.17%	2.12%	2.48%	0.52%
S5	4.71%	0.86%	1.42%	0.31%
S6	4.1%	0.78%	0.31%	0.33%
S7	2.57%	0.43%	0.64%	0.29%
S8	1.92%	1.64%	1.65%	0.38%
S9	0.18%	3.66%	4.32%	0.49%
AVG	2.72%	1.33%	1.56%	0.36%

LiRT has the highest errors in most specimens, making it the least effective model for toughness prediction based on the lowest average error percentage. Overall, PRT + ANN emerges as the most effective model for toughness prediction based on the lowest average error percentage as displayed in Fig. 7.

Moreover, the prediction uncertainty

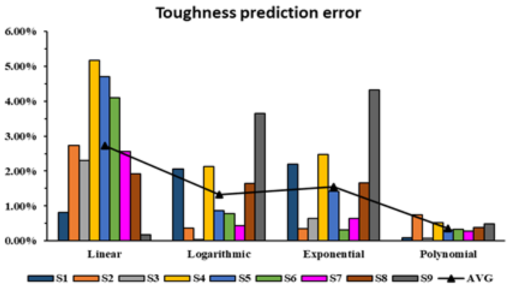

Fig. 7. Graph of toughness prediction error from regression.

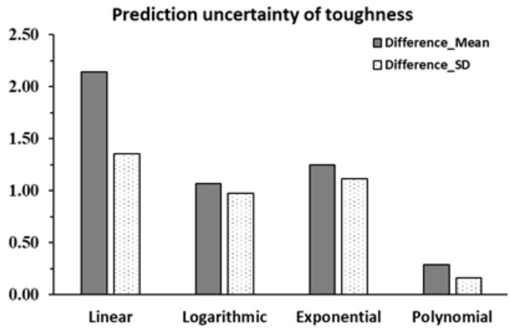

Fig. 8. Prediction uncertainty of toughness.

analysis for the Toughness values across different regression models—Linear, Logarithmic, Exponential, and Polynomial—was evaluated using the mean difference (Difference_Mean) and standard deviation of the difference (Difference_SD) between the actual and predicted values.

As shown in Fig. 8, among the four models, the Polynomial model demonstrated the highest prediction accuracy, with the lowest mean difference of 0.2849 and standard deviation of 0.1622, indicating both low bias and high consistency in predictions. The Logarithmic model followed with a mean difference of 1.0687 and a standard deviation of 0.9725, while the Exponential model showed a slightly higher mean difference of 1.2467 and standard deviation of 1.1163. The Linear model exhibited the highest uncertainty, with a mean difference of 2.1438 and standard deviation of 1.3555.

These results highlight that the Polynomial model provides the most reliable predictions for Toughness, with the narrowest prediction spread and minimal deviation from actual values, making it the most suitable model in terms of prediction uncertainty. The LIME contribution analysis for toughness prediction across different regression models reveals how each input feature influences the predicted values. For the Linear model, the Temp feature contributed +2.53 and Holding Time (HT) +2.10, leading to a total contribution of +4.33 and a predicted value of 78.80, within a range of 66.07–88.01. In the Exponential model, both Temp and HT added +2.53 and +2.47 respectively, with a combined contribution of +5.00, predicting 80.53 (range: 67.97–91.45). The Logarithmic model showed slightly higher contributions of +2.78 for Temp and +3.30 for HT, totaling +6.08 with a prediction of 81.53 (range: 67.89–88.75). Lastly, the Polynomial model had the highest individual impacts—+3.40 from Temp and +3.09 from HT—summing to +6.49 and resulting in a predicted value of 82.06, bounded by 66.94–87.08. These findings illustrate how different regression approaches vary in feature influence and prediction confidence. Table 7 exhibits Lime contribution toughness.

3.2 Hardness prediction

The comparison of hardness predictions highlights that LiRH and PRH are the most effective models for predicting values close to the experimental target of 34. The first prediction using Pure data+Duplication+ANN results in a slightly underestimated value of 33.23, a range of difference of -2.26%. Among the only regression models from RBDP, LiRH provides a prediction of 34.26 (0.76%), which

Table 7. LIME contribution for toughness.

LIME Contribution for Toughness				
Features	**Linear**	**Expo.**	**Log.**	**Polynom.**
Temp	2.53	2.53	2.78	3.4
HT	2.1	2.47	3.3	3.09
Total Con.	4.33	5	6.08	6.49
Pred. Value	78.8	80.53	81.53	82.06
Pred. Range	66.07 - 88.01	67.97 - 91.45	67.89 - 88.75	66.94 - 87.08

Table 8. Comparison of hardness prediction results from each method.

Exp.		**Pure data + Duplication + ANN**	**RBDP only**				**RBDP+ANN**			
			LiRH	ERH	LoRH	PRH	LiRH	ERH	LoRH	PRH
S9	34	33.23	34.26	34.48	35.81	34.33	34.59	33.23	35.1	34.24
Diff	-	-2.26%	0.76%	1.41%	5.32%	0.97%	1.74%	-2.26%	3.24%	0.71%

is close to the target, while ERH and LoRH yield predictions of 34.48 (1.41%) and 35.81 (5.32%), respectively, both near the target but slightly above it. PRH overestimates with a prediction of 34.33 (0.97%), making it less suitable. In combined ANN approaches, PRH changes to provide the best prediction value as 34.24 (0.71%), aligning closely with the target and demonstrating effective performance. Overall, PRH + ANN proves to be the most effective model for achieving predictions that closely match the experimental target value of 34 as shown in Table 8.

Moreover, as shown in Table 9, the prediction error results for hardness from different regression models from RBDP (LiRH, ERH, LoRH, PRH) across the target dataset including nine specimens (S1-S9). Across the nine specimens, PRH consistently delivers the most accurate predictions, achieving the lowest average error of 0.72%. It performs particularly well for Specimens 1, 3, 4, and 9, making it the most reliable model overall. LoRH, while occasionally performing best (e.g., in Specimens 5-8), tends to have higher errors, especially for Specimens 1, 2, and 4, resulting in the highest average error at 2.05%. LiRH and ERH offer moderate accuracy, with LiRH performing exceptionally for Specimen 2 (0.01%) but falling short in others. PRH+ANN emerges as the most effective model for hardness prediction based on the lowest average error percentage as Fig. 9. Moreover, the prediction uncertainty analysis for Hardness was evaluated using the mean difference and standard deviation (SD) between actual and predicted values across four regression models: Linear, Logarithmic, Exponential, and Polynomial. As exhibited in Fig. 10, the Polynomial model outperformed the others, showing the lowest prediction error, with a Difference_Mean of 0.2006 and a Difference_SD of 0.0995, indicating high accuracy and precision. In contrast, the Exponential model exhibited the highest prediction uncertainty, with a Difference_Mean of 0.5298 and Difference_SD of 0.4264, followed by the Logarithmic and Linear models with similar performance (Difference_Mean around 0.52 and SD between 0.31 and 0.36). These findings suggest that the Polynomial model provides the most reliable and consistent predictions for Hardness, with minimal deviation from actual values, making it the most appropriate

Table 9. Comparison on hardness prediction error results from regression.

Specimens	LiRH	ERH	LoRH	PRH
S1	2.47%	5.24%	4.45%	1.01%
S2	0.01%	3.36%	0.09%	0.33%
S3	1.54%	1.91%	1.62%	0.41%
S4	4.47%	3.26%	4.39%	1.27%
S5	1.43%	0.86%	1.14%	1.16%
S6	1.83%	0.77%	1.19%	0.36%
S7	1.41%	0.35%	0.6%	0.44%
S8	1.67%	0.44%	0.8%	0.79%
S9	1.72%	2.25%	3.23%	0.72%
AVG	1.84%	2.05%	1.95%	0.72%

model in terms of prediction certainty and stability.

The LIME contribution analysis for hardness prediction across different regression models shows varying impacts of the input features, Temperature (Temp) and Holding Time (HT), on the predicted outcomes. In the Linear model, Temp contributed +1.55 and HT +1.64, resulting in a total contribution of +3.18 and a predicted value of 20.82, within a range of 20.82–34.71. The Exponential model showed slightly lower influence, with Temp at +1.50 and HT at +1.37, totaling +2.88, predicting 21.34 with a range of 21.34–35.40. The Logarithmic model presented a stronger HT influence (+2.14) and Temp at +1.37, giving a total of +3.51 and a prediction of 29.54 within 21.04–35.52. Lastly, the Polynomial model had Temp and HT contributions of +1.54 and +1.44 respectively, with a total of +2.98 and a prediction of 29.17 within 21.16–34.64. These results highlight how each regression model assigns different levels of importance to the same features, impacting both the predicted hardness values and the associated uncertainty ranges. Table 10 demonstrates Lime contribution hardness.

Table 10. LIME contribution for hardness.

LIME Contribution for Hardness				
Features	**Linear**	**Expo.**	**Log.**	**Polynom.**
Temp	1.55	1.50	1.37	1.54
HT	1.64	1.37	2.14	1.44
Total Con.	3.18	2.88	3.51	2.98
Pred. Value	20.82	21.34	29.54	29.17
Pred. Range	20.82 - 34.71	21.34 - 35.40	21.04 - 35.52	21.16 - 34.64
Pred. Range	20.82 - 34.71	21.34 - 35.40	21.04 - 35.52	21.16 - 34.64

3.3 ANN architecture for sensitivity analysis

In this section, the results of the sensitivity analysis on Artificial Neural Network (ANN) architecture are presented. The study focuses on examining how variations in activation functions, the number of hidden layers, and the number of neurons influence the prediction error for mechanical properties as shown in tables in the Appendix. By systematically adjusting these parameters, the impact on the performance of regression models for toughness and hardness was analyzed. The findings highlight the importance of selecting appropriate architectural configurations to achieve the lowest possible prediction errors.

For the prediction of toughness, the best configuration and activation function for each regression model was identified. The Linear regression model achieved the minimum error of 2.44% using the Swish activation function with 4 hidden layers and 128 neurons. The Logarithmic model showed its best performance with a 0.91% error using the Sigmoid activation function, also with 4 hidden layers and 128 neurons. For the Exponential model, the optimal solution was obtained with the Sigmoid activation, 2 hidden layers, and 128 neurons, achieving a 0.92% error. The Polynomial model achieved the lowest error of 0.58% using the Swish activation function with 6 hidden layers and 128 neurons.

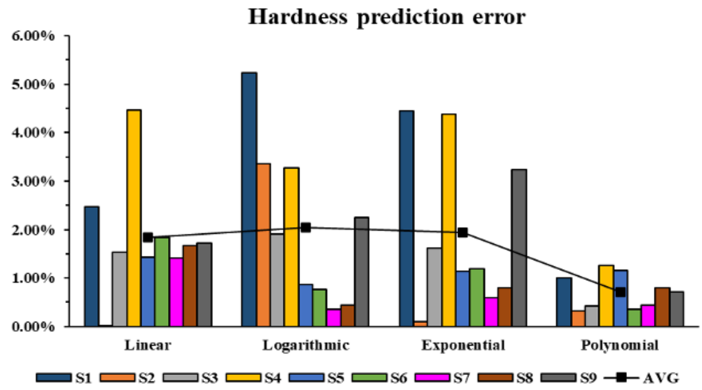

Fig. 9. Graph of hardness prediction error results from regression.

Table 11. Results of artificial neural network (ANN) architecture.

Mechanical properties	Regression models	Best solution			Minimum error	Appendix
		Activations	Configuration			
			No. of hidden layers	No. of neurons		
Toughness	Linear	Swish	4	128	2.44%	Table. 16
	Logarithmic	Sigmoid	4	128	0.91%	Table. 17
	Exponential	Sigmoid	2	128	0.92%	Table. 18
	Polynomial	Swish	6	128	0.58%	Table. 19
Hardness	Linear	Swish	2	128	1.2%	Table. 20
	Logarithmic	Sigmoid	2	64	1.12%	Table. 21
	Exponential	Swish	6	128	1.36%	Table. 22
	Polynomial	ReLU	2	128	0.72%	Table. 23

Table 12. Comparison of ML models for toughness prediction.

Feature		Target Toughness	ML models							
Temp (°C)	HT (min)		ANN + Polynomial		SVR		RF		XGBoost	
			Predict	Error	Predict	Error	Predict	Error	Predict	Error
760	2	67	66.94	0.09%	67.58	0.87%	66.98	0.03%	66.98	0.03%
760	4	71	70.46	0.75%	70.61	0.55%	70.51	0.69%	70.52	0.68%
760	6	73	72.95	0.07%	72.99	0.01%	72.89	0.15%	72.9	0.14%
800	2	78	77.59	0.52%	77.48	0.67%	77.48	0.67%	77.43	0.73%
800	4	80	80.25	0.31%	80.11	0.14%	80.15	0.19%	80.34	0.43%
800	6	82	81.73	0.33%	81.58	0.51%	81.68	0.39%	81.63	0.45%
840	2	84	83.76	0.29%	83.74	0.31%	83.84	0.19%	83.83	0.2%
840	4	86	85.67	0.38%	85.55	0.52%	85.65	0.41%	85.65	0.41%
840	6	87	87.42	0.49%	81.65	6.15%	85.65	1.55%	85.7	1.49%

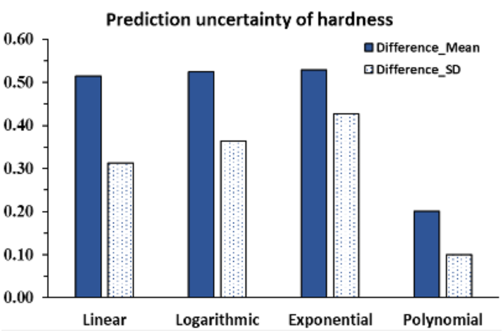

Fig. 10. Prediction uncertainty of hardness.

Regarding hardness, the Linear model performed best with the Swish activation, 2 hidden layers, and 128 neurons, resulting in a 1.20% error. The Logarithmic model achieved its minimum error of 1.12% using the Sigmoid activation with 2 hidden layers and 64 neurons. The Exponential model reached its best result with a 1.36% error using the Swish activation, 6 hidden layers, and 128 neurons. Finally, the Polynomial model showed the best performance with a 0.72% error using the ReLU activation function, 2 hidden layers, and 128 neurons. Table 11 shows results of ANN architecture.

The results confirm that the Polynomial regression model consistently provided the best performance for both toughness and hardness, achieving the lowest prediction errors among all models tested.

3.4 Comparison of ML models

This study includes a comparative analysis of multiple machine learning (ML) models—specifically Artificial Neural Networks (ANN), Support Vector Regression (SVR), Random Forest (RF), and XGBoost. Although ANN models have shown promising results in prior studies for predicting material properties, relying solely on a single model may introduce bias or overfitting, especially with limited or nonlinear datasets. By comparing the performance of ANN with other widely used models such as SVR (known for handling high-dimensional data), RF (known for stability and resistance to overfitting), and XGBoost (recognized for its optimization and boosting techniques), this research ensures a more comprehensive evaluation.

Table 12 presents a comparative analysis of predicted toughness values and corresponding percentage errors for different machine learning models, including Artificial Neural Networks with Polynomial features (ANN + Polynomial), Support Vector Regression (SVR), Random Forest (RF), and XGBoost. The models were evaluated on a new dataset consisting of various heat treatment conditions defined by temperature and holding time. The target variable is the actual toughness observed from experimental data. As shown in Fig. 11, all models yield low error percentages under most conditions. However, SVR shows a relatively high deviation of 6.15% in predicting toughness at 840°C with 6 minutes holding time, whereas other models maintain errors below 2%. Among the evaluated models, ANN + Polynomial and Random Forest consistently deliver the most accurate predictions with minimal percentage error across all test cases.

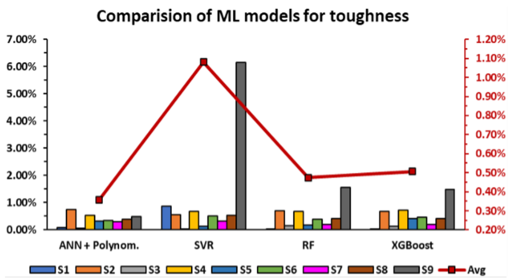

Fig. 11. Graph of toughness prediction error results with several ML models.

Fig. 11. exhibits graph of toughness prediction error results with several ML models. Table 13 provides a detailed comparison between the actual and predicted hardness values obtained from four machine learning models: Artificial Neural Networks with Polynomial Features (ANN + Polynomial), Support Vector Regression (SVR), Random Forest (RF), and XGBoost. The data consists of different temperature and time combinations used as input features, with hardness values as the target. The results indicate that ANN combined with Polynomial features, Random Forest (RF), and XGBoost exhibit high accuracy in predicting material hardness, consistently maintaining prediction errors below 1% across most conditions. While Support Vector Regression (SVR) performs similarly in many cases, it shows a substantial error of 11.47% under the highest temperature and longest holding time (840°C, 6 min), suggesting a sensitivity to extreme or

Table 13. Comparison of ML models for hardness prediction.

Feature		Target Hardness	ML models							
Temp (°C)	HT (min)		ANN + Polynom.		SVR		RF		XGBoost	
			Predict	Error	Predict	Error	Predict	Error	Predict	Error
760	2	21	21.21	1.01%	21.16	0.76%	21.06	0.29%	21.07	0.33%
760	4	23	22.93	0.33%	22.97	0.13%	22.87	0.57%	22.88	0.52%
760	6	25	24.9	0.41%	24.92	0.32%	24.82	0.72%	24.83	0.68%
800	2	27	26.66	1.27%	26.51	1.81%	26.52	1.78%	26.5	1.85%
800	4	28	28.32	1.16%	28.2	0.71%	28.2	0.71%	28.31	1.11%
800	6	30	29.89	0.36%	29.91	0.3%	30.01	0.03%	29.98	0.07%
840	2	31	31.14	0.44%	31.04	0.13%	31.14	0.45%	31.13	0.42%
840	4	33	32.74	0.79%	32.56	1.33%	32.66	1.03%	32.66	1.03%
840	6	34	34.24	0.72%	30.1	11.47%	32.66	3.94%	32.77	3.62%

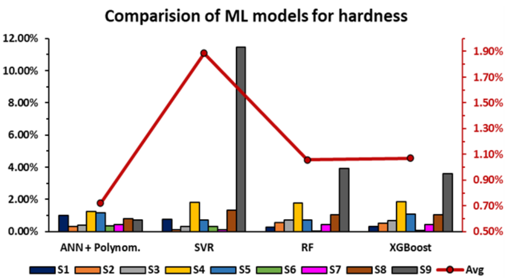

Fig. 12. Graph of hardness prediction error results with several ML models.

extrapolated input values. Among all models, Random Forest and ANN + Polynomial demonstrate the lowest average errors and most consistent performance, highlighting their robustness and reliability. These findings suggest that tree-based models and polynomial-enhanced neural networks are particularly effective for modeling material properties under diverse heat treatment scenarios, making them preferable choices for this type of predictive task. Fig. 12 represents graph of hardness prediction error results with several ML models.

3.5 Statistical validation for regression model

The performance of different regression models for predicting toughness is summarized in the table below. The values for various performance metrics, including RMSE, MAE, WMAPE, MAPE, PI, RSR, NS, and VAF, were compared to assess the effectiveness of each regression model. As listed in Table 14, among the regression models tested, the Polynomial model consistently achieved the lowest error metrics (RMSE, MAE, WMAPE, MAPE) and the highest values for PI, NS, and VAF, making it the best performing model across all measures.

Table 15 exhibits Statistical validation hardness, Similar to the toughness results, the Polynomial model achieved the lowest error metrics (RMSE, MAE, WMAPE, MAPE) and the highest values for PI, NS, and VAF, making it the best performing model across all measures for predicting hardness.

4. Discussion

This study proposes a significant contribution by introducing the Regression Preforming RBDP method, which enhances the performance of ANNs in predicting the mechanical properties of DP steel, specifically toughness and hardness.

Existing studies, such as those by Ersoy et al. [1] and Kuang et al. [2], primarily focus on the influence of microstructure and thermal treatments on the mechanical properties of DP steel, with limited exploration into predictive modeling approaches. While these works provide valuable experimental insights, they do not incorporate advanced data-driven methodologies for pre-

Table 14. Statistical validation for toughness.

Regression	Regular performance measurements for toughness							
	RMSE (Lowest)	MAE (Lowest)	WMAPE (Lowest)	MAPE (Lowest)	PI (Highest)	RSR (Lowest)	NS (Highest)	VAF (Highest)
Linear	2.4958	2.1438	2.7251	2.7219	100	0.3565	0.857	95.9155
Logarithmic	1.4081	1.0687	1.3585	1.3302	100	0.2012	0.9545	95.8126
Exponential	1.6315	1.2467	1.5848	1.5552	100	0.2331	0.9389	94.36
Polynomial	0.3233	0.2849	0.3621	0.3587	100	0.0462	0.9976	99.8023
Best Value	0.3233	0.2849	0.3621	0.3587	All	0.0462	0.9976	99.8023
Best Regression	Polynomial	Polynomial	Polynomial	Polynomial	All	Polynomial	Polynomial	Polynomial

Table 15. Statistical validation for hardness.

Regression	Regular performance measurements for hardness							
	RMSE (Lowest)	MAE (Lowest)	WMAPE (Lowest)	MAPE (Lowest)	PI (Highest)	RSR (Lowest)	NS (Highest)	VAF (Highest)
Linear	0.594	0.5151	1.8395	1.8388	100	0.1337	0.9799	98.4039
Logarithmic	0.6276	0.5249	1.8748	2.0502	100	0.1412	0.9776	97.7565
Exponential	0.665	0.5298	1.8921	1.945	100	0.1496	0.9748	97.5154
Polynomial	0.2214	0.2006	0.7164	0.7199	100	0.0498	0.9972	99.7207
Best Value	0.2214	0.2006	0.7164	0.7199	All	0.0498	0.9972	99.7207
Best Regression	Polynomial	Polynomial	Polynomial	Polynomial	All	Polynomial	Polynomial	Polynomial

dictive accuracy.

In contrast, studies like Omid et al. [7] and Ghosh et al. [9] applied machine learning techniques, but their focus is on the optimization of mechanical properties using response surface methodology. These studies lack a comprehensive data preprocessing strategy that could improve model performance, particularly for ANNs. The RBDP method presented in this study addresses this gap by employing synthetic data generation and dataset expansion, providing ANNs with a more diverse and representative training dataset. This approach potentially captures nuanced relationships between intercritical annealing parameters and mechanical properties that might be overlooked by traditional models.

Furthermore, this study aligns with the growing trend of materials informatics and big data, as highlighted by Agrawal and Choudhary [10], where comprehensive datasets are essential for improving model performance. By comparing the RBDP-enhanced ANN with traditional regression models and pure ANNs, this research demonstrates that the RBDP method significantly improves prediction accuracy. This contribution fills a critical gap in current literature by offering a robust preprocessing technique tailored for ANN-based predictions, outperforming traditional models and providing a new direction for the application of machine learning in materials science.

5. Conclusion

This study presents a novel data preprocessing method, the Regression-Based Data Preprocessing (RBDP) technique, to enhance the performance of Artificial Neural Networks (ANNs) in predicting the mechanical properties of dual-phase (DP) steel, specifically toughness and hardness. By generating synthetic data and expanding the dataset through regression analysis, RBDP improves the accuracy of ANN predictions, addressing limitations of both traditional regression models and pure ANNs. The results of this study demonstrate that RBDP-enhanced ANNs significantly outperform traditional models in predicting mechanical properties, particularly when dealing with the nonlinear and complex relationships between intercritical annealing parameters and the mechanical properties of DP steel. For toughness prediction, the RBDP method, particularly the LiRT + ANN model, provided the most accurate predictions, closely matching experimental values with minimal error. Similarly, for hardness prediction, the PRH + ANN model was found to deliver the most accurate results, demonstrating its effectiveness in aligning predictions with experimental targets. However, PRH + ANN is the most accurate model for hardness and toughness prediction, both showing superior performance in aligning predictions with experimental data. Overall, the RBDP method provides a robust and efficient approach for enhancing ANN-based predictions of DP steel properties, filling a critical gap in current modeling techniques. This method can be further explored and applied to other materials and processing conditions, paving the way for more accurate and reliable predictive models in materials science.

Future research could focus on implementing the Regression-Based Data Preprocessing (RBDP) method in real-time applications to enhance prediction accuracy for extrapolating mechanical properties of dual-phase (DP) steel. By incorporating new data and updating the model with synthetic data based on regression trends, the model could adapt to unseen process conditions without full retraining. This approach would improve the model's ability to generalize to novel parameter combinations, increasing prediction reliability in dynamic manufacturing environments.

Acknowledgements

The authors acknowledge their gratitude to Valaya Alongkorn Rajabhat University under the Royal Patronage, and Rajamangala University of Technology Thanyaburi for providing the research facilities.

References

[1] Ersoy N, Kuang CF, Calcagnotto M, Kadkhodapour J, Tavares SSM, Ali M, et al. Microstructure and mechanical properties of dual phase steels. Mater Sci Eng A. 2015; 627:260-73.

[2] Kuang CF, Ersoy N, Calcagnotto M, Kadkhodapour J, Tavares SSM, Ali M, et al. Effects of quenching and tempering on the microstructure and mechanical properties of a medium-carbon dual-phase steel. Mater Sci Eng A. 2014; 613:178-83.

[3] Calcagnotto M, Kadkhodapour J, Tavares SSM, Ali M. Deformation and fracture mechanisms in fine- and ultrafine-grained ferrite/martensite dual-phase steels and the effect of aging. Acta Mater. 2011;59(2):658-70.

[4] Kadkhodapour J, Calcagnotto M, Tavares SSM, Ali M. Experimental and numerical study on geometrically necessary dislocations and non-homogeneous mechanical properties of the ferrite phase in dual phase steels. Acta Mater. 2011;59(11):4387-94.

[5] Tavares SSM, Calcagnotto M, Kadkhodapour J, Ali M. Microstructure and mechanical properties of a dual phase steel. Mater Charact. 2011;62(7):698-705.

[6] Ali M, Calcagnotto M, Kadkhodapour J, Tavares SSM. Effect of double annealing on mechanical properties of dual phase steel. J Mater Eng Perform. 2014;23(9):3233-40.

[7] Omid G, Kadkhodapour J, Tavares SSM, Ali M. Optimization of the mechanical properties of dual-phase steels using response surface methodology. Mater Des. 2016; 103:330-6.

[8] Singh J, Calcagnotto M, Kadkhodapour J, Tavares SSM, Ali M. Influence of intercritical annealing parameters on the mechanical properties of medium carbon dual phase steel. Mater Today Proc. 2018;5(2):7748-57.

[9] Ghosh A, Omid G, Kadkhodapour J, Ali M. Optimization of mechanical properties of dual phase steels using artificial neural network. Mater Des. 2016; 106:490-7.

[10] Agrawal A, Choudhary A. Perspective: Materials informatics and big data: Realization of the 'fourth paradigm' of science in materials science. APL Mater. 2016;4(5):053208.

[11] Liu Y, Calcagnotto M, Kadkhodapour J, Tavares SSM. Machine learning for the prediction of mechanical properties of metals. NPJ Comput Mater. 2020;6(1):1-17.

[12] Bhadeshia HKDH. Neural networks in materials science. ISIJ Int. 2019;59(6):934-42.

[13] Conduit BD, Calcagnotto M, Kadkhodapour J, Tavares SSM. Design of a nickel-base superalloy using a neural network. Mater Des. 2017; 131:358-65.

[14] Wen C, Kadkhodapour J, Tavares SSM, Calcagnotto M. Machine learning assisted design of high entropy alloys with desired property. Acta Mater. 2019; 170:109-17.

[15] Agrawal A, Choudhary A. Perspective: Materials informatics and big data: Realization of the "fourth paradigm" of science in materials science. APL Mater. 2016;4(5):053208.

[16] Liu Y, Zhao T, Ju W, Shi S. Materials discovery and design using machine learning. J Materiomics. 2017;3(3):159-77.

[17] Jha R, Dulikravich GS, Chakraborti N, Fan M, Schwartz J, Koch CC, et al. Algorithms for design optimization of chemistry of hard magnetic alloys using experimental data. J Alloys Compd. 2016; 682:454-67.

[18] Agarwal H, Gokhale AM, Graham S, Horstemeyer MF. Void growth in 6061-aluminum alloy under triaxial stress state. Mater Sci Eng A. 2003;341(1-2):35-42.

[19] Singh RR, Gaikwad A, Singh SS, Singh VP. Comparison of mechanical properties of medium carbon steel with dual phase steel. Int J Mech Eng. 2015;4(4):1-8.

[20] Patki N, Wedge R, Veeramachaneni K. The synthetic data vault. 2016 IEEE International Conference on Data Science and Advanced Analytics (DSAA); 2016. p. 399-410.

[21] Xu L, Skoularidou M, Cuesta-Infante A, Veeramachaneni K. Modeling tabular data using conditional GAN. Adv Neural Inf Process Syst. 2019;32.

[22] Chawla NV, Bowyer KW, Hall LO, Kegelmeyer WP. SMOTE: Synthetic Minority Over-sampling Technique. J Artif Intell Res. 2002; 16:321-57.

[23] Shorten C, Khoshgoftaar TM. A survey on image data augmentation for deep learning. J Big Data. 2019;6(1):60.

Appendix

Table 16. Error of toughness using linear.

ANN Architecture				Error of Toughness using Linear (%)										Best (Minimum)	
				S1	S2	S3	S4	S5	S6	S7	S8	S9	AVG	Config.	Activation
ReLU	2	32	C1	0	3.73	3.88	7.08	5.94	5.61	5.47	4.73	2.66	4.34	2.72	2.72
		64	C2	1.43	4.22	3.7	5.89	5.6	5.07	5.25	5.29	2.65	4.34		
		128	C3	0.81	2.73	2.3	5.17	4.71	4.1	2.57	1.92	0.18	2.72		
	4	32	C4	0.05	3.35	2.9	6.74	4.69	5.28	4.97	5.48	5.07	4.28	2.88	
		64	C5	3.66	0.48	0.39	4.07	3.92	4.02	4.14	3.38	1.83	2.88		
		128	C6	0.78	2.26	2.55	4.95	4.11	3.81	3.25	3.48	2.4	3.06		
	6	32	C7	1.67	2.54	2.42	4.78	4.83	2.98	3.12	3.42	2.63	3.15	2.87	
		64	C8	2.5	2.03	2.58	5.06	5.56	4.14	3.47	4.78	4.45	3.84		
		128	C9	1.58	2.08	2.11	5.25	4.5	2.75	2.1	2.87	2.57	2.87		
Sigmoid	2	32	C10	0.6	3.45	2.65	5.41	4.67	3.17	1.99	2.18	2.58	2.97	2.97	2.97
		64	C11	0.7	3.61	2.2	5.31	4.12	3.43	2.92	2.81	2.85	3.11		
		128	C12	0.91	3.03	2.24	5.71	5.01	3.56	2.59	2.51	3.43	3.22		
	4	32	C13	0.94	4	2.88	5.79	5.13	5.12	4.19	4.57	5.23	4.2	3.07	
		64	C14	0.11	3.58	2.32	5.05	4.12	3.74	2.79	2.59	3.32	3.07		
		128	C15	1.26	3.61	2.35	5.72	4.46	3.62	2.53	2.02	2.74	3.14		
	6	32	C16	0.68	4.65	3.05	6.33	5.22	3.71	2.15	3.87	4.93	3.85	3.39	
		64	C17	0.07	3.27	3.02	6.24	5.29	4.43	4.15	3.63	4.41	3.83		
		128	C18	0.43	3.61	2.11	5.04	5	4.28	3.1	2.92	4.03	3.39		
Swish	2	32	C19	1.83	3.96	3.1	5.78	4.85	4.11	3.45	3.53	3.38	3.78	2.96	2.44
		64	C20	0.14	2.68	2.11	5.28	4.4	3.74	3.17	3.12	2.25	2.99		
		128	C21	1.47	3.4	2.35	5.61	4.47	3.46	2.96	2.28	0.66	2.96		
	4	32	C22	0.74	3.02	1.86	5.28	4.31	3.37	2.43	2.39	3.28	2.96	2.44	
		64	C23	2.12	4.16	2.97	5.22	4.33	3.84	3.05	3.24	3.05	3.55		
		128	C24	1.6	3.84	2.71	5.32	3.79	2.42	1.32	0.81	0.1	2.44		
	6	32	C25	0.5	3.78	3.12	5.88	5.03	3.81	2.04	2.16	3.05	3.26	2.92	
		64	C26	0.92	3.19	2.98	5.4	4.42	3.31	1.47	1.76	2.83	2.92		
		128	C27	2.09	4.49	2.79	4.91	3.66	2.94	3.09	3.76	4.72	3.6		

Table 17. Error of toughness using logarithmic.

ANN Architecture				Error of Toughness using Logarithmic (%)										Best (Minimum)	
				S1	S2	S3	S4	S5	S6	S7	S8	S9	AVG	Config.	Activation
ReLU	2	32	C1	3.92	0.2	0.12	2.65	1.22	2	0.79	0.16	1.77	1.43	1.33	1.17
		64	C2	1.63	1.54	1.83	3.76	2.34	2.96	1.93	1.47	1	2.05		
		128	C3	2.06	0.38	0.04	2.12	0.86	0.78	0.43	1.64	3.66	1.33		
	4	32	C4	3.46	0.08	0.63	3.84	1.74	2	2.48	0.38	1.67	1.81	1.17	
		64	C5	3.47	0.63	0.15	3.1	0.56	1.1	0.1	0.11	1.28	1.17		
		128	C6	6.87	3.21	2.54	1.42	1.27	2.02	0.54	0.95	1.87	2.3		
	6	32	C7	5.59	1.4	0.58	2.58	2.49	1.44	1.33	1.26	1.36	2	1.81	
		64	C8	6.92	2.47	1.3	1.6	1.55	2.3	0.15	1.36	1.48	2.13		
		128	C9	6.09	2.28	1.45	1.12	1.62	0.55	0.42	1.48	1.25	1.81		
Sigmoid	2	32	C10	3.24	0.4	0.28	2.72	2.64	2.35	1.86	1.19	1.2	1.77	1.02	0.91
		64	C11	1.7	0.74	0.14	2.49	1.85	1.63	0.64	0.79	1.15	1.24		
		128	C12	2.49	1.22	1.44	1.62	0.8	0.82	0.29	0.16	0.39	1.02		
	4	32	C13	3.68	0.73	0.67	2.28	1.14	0.61	0.36	0.76	0.08	1.15	0.91	
		64	C14	3.1	0.42	0.01	2.38	1.16	0.89	0.18	0.09	0.46	0.96		
		128	C15	1.86	0.46	0.28	2.31	1.26	0.74	0.19	0.68	0.43	0.91		
	6	32	C16	3.96	1.64	0.16	2.43	1.79	1.38	0.02	0.61	1.68	1.52	1.21	
		64	C17	3.26	1.75	0.81	1.94	0.99	0.77	0.35	0.47	0.53	1.21		
		128	C18	2.7	0.73	0.54	1.7	1.29	1.3	1.81	0.83	0.3	1.25		
Swish	2	32	C19	3.5	0.56	0.49	2.53	2.3	2.06	0.92	0.54	0.52	1.49	1.13	0.99
		64	C20	2.81	0.37	0.13	2.13	0.88	0.79	0.22	0.96	1.88	1.13		
		128	C21	2.9	1.61	1.91	1.23	0.44	0.81	1.57	2.56	3.06	1.79		
	4	32	C22	2.78	0.36	0.39	3.14	2.33	2.14	1.06	0.86	0.36	1.49	0.99	
		64	C23	4.34	1.29	0.96	2.13	1.91	2.22	1.51	1.44	1.53	1.93		
		128	C24	2.54	0.27	0.62	1.87	0.51	0.22	0.95	1.12	0.8	0.99		
	6	32	C25	3.99	0.43	0.61	3.84	2.98	2.07	0.79	1.46	2.59	2.08	1.52	
		64	C26	3.53	0.99	0.98	3.54	1.82	0.29	1.22	2.6	2.7	1.96		
		128	C27	1.65	1.14	1.04	4.31	2.48	0.54	0.29	1.11	1.13	1.52		

Table 18. Error of toughness using exponential.

ANN Architecture				Error of Toughness using Exponential (%)										Best (Minimum)	
				S1	S2	S3	S4	S5	S6	S7	S8	S9	AVG	Config.	Activation
		32	**C1**	2.74	1.2	0.7	3.47	2.61	1.82	1.23	0.04	2.55	1.82	1.82	1.41
	2	**64**	**C2**	3.79	0.47	1.07	4.08	1.89	2.27	0.28	0.36	2.69	1.88		
		128	**C3**	2.19	0.35	0.64	2.48	1.42	0.31	0.64	1.65	4.32	1.56		
		32	**C4**	6.12	1.79	1.6	3.22	1.15	0.42	0.18	0.36	0.61	1.71	1.71	
ReLU	**4**	**64**	**C5**	4.75	0.73	0.17	4	3.88	3.81	1.49	2.12	1.61	2.51		
		128	**C6**	5.44	1.74	1.28	1.51	1.32	1.2	2.14	2.3	4.21	2.35		
		32	**C7**	4.34	0.01	1.36	4.45	2.82	1.66	1.37	2.11	1.73	2.21	1.41	
	6	**64**	**C8**	5.18	0.79	0.07	3.29	2.42	0.2	0.72	1.08	0.23	1.55		
		128	**C9**	4.97	1.45	1.37	1.51	1.77	0.26	0.54	0.17	0.61	1.41		
		32	**C10**	3.91	0.03	0.58	2.6	1.85	0.87	0.27	0.39	0.54	1.23	0.92	0.92
	2	**64**	**C11**	3.25	0.52	0.28	2.62	1.88	0.54	1.06	1.5	1.8	1.49		
		128	**C12**	1.47	0.4	0.01	2.43	1.75	1.1	0.65	0.12	0.4	0.92		
		32	**C13**	4.48	0.82	0.7	2.16	0.75	0.36	1.62	1.16	0.3	1.37	1.29	
Sigmoid	**4**	**64**	**C14**	3.56	0.72	0.77	2.18	1.04	0.51	1.35	1.01	0.46	1.29		
		128	**C15**	1.84	1.54	0.27	3.18	2.18	2.11	0.29	0.68	0.46	1.4		
		32	**C16**	4.62	1.04	0.06	3.24	2.11	1.48	0.23	1.43	2.46	1.85	1.39	
	6	**64**	**C17**	3.73	0.58	0.19	2.65	2.05	2.18	1.35	0.62	1.26	1.62		
		128	**C18**	2.65	0.7	1.58	2.89	1.68	0.83	0.61	1.34	0.18	1.39		
		32	**C19**	3.28	0.07	0.64	3.02	1.8	0.08	0.84	0.63	1.41	1.31	1.31	1.31
	2	**64**	**C20**	1.61	0.75	0.55	3.43	1.46	0.47	0.58	2.02	4.09	1.66		
		128	**C21**	1.81	0.73	0.07	3.2	1.88	0.45	0.47	1.82	4.2	1.62		
		32	**C22**	3.14	0.43	0.12	2.58	1.79	0.8	1.09	1.15	1.17	1.36	1.36	
Swish	**4**	**64**	**C23**	4.32	0.34	0.6	2.88	1.71	0.63	0.21	0.37	1.77	1.43		
		128	**C24**	0.45	1.47	0.11	4.01	2.28	0.65	0.35	0.92	2.87	1.46		
		32	**C25**	4.76	0.4	0.51	2.6	1.47	0.04	1.62	1.32	0.41	1.46	1.46	
	6	**64**	**C26**	4.97	0.65	0.36	2.86	1.52	0.34	2.38	2.12	1.18	1.82		
		128	**C27**	5.48	2.4	2.54	2.05	1.55	0.9	1.38	1.41	1	2.08		

Table 19. Error of toughness using polynomial.

ANN Architecture				Error of Toughness using Polynomial (%)										Best (Minimum)	
				S1	S2	S3	S4	S5	S6	S7	S8	S9	AVG	Config.	Activation
		32	**C1**	1.98	0.37	0.97	1.69	0.38	1.4	0.24	0.8	0.05	0.88	0.36	0.75
	2	**64**	**C2**	1.07	0.44	1.54	0.92	0.61	0.39	1.25	0.34	3.59	1.13		
		128	**C3**	0.09	0.75	0.07	0.52	0.31	0.33	0.29	0.38	0.49	0.36		
		32	**C4**	4.39	1.35	1	0.41	0.49	0.37	0.59	0.13	0.36	1.01	1.01	
ReLU	**4**	**64**	**C5**	2.51	0.86	0.69	0.53	1.68	1.31	2.24	3.4	3.84	1.89		
		128	**C6**	2.7	0.45	0.12	1.59	1	1.5	2.02	2.93	2.82	1.68		
		32	**C7**	1.25	0.68	0.62	0.64	0.35	0.89	1.8	3.42	3.77	1.49	0.75	
	6	**64**	**C8**	0.87	0.04	0.22	2.98	0.19	0.33	0.01	0.99	1.14	0.75		
		128	**C9**	4.99	1.8	0.73	0.26	0.12	0.81	0.73	0.92	2.23	1.4		
		32	**C10**	1.58	1.63	0.64	0.76	0.78	0.71	0.3	1.38	2.09	1.1	0.79	0.78
	2	**64**	**C11**	1.76	0.14	1.05	0.61	0.48	0.11	0.26	0.87	1.82	0.79		
		128	**C12**	0.26	1.45	0.86	0.63	0.21	0.53	0.6	1.31	2.26	0.9		
		32	**C13**	2.11	1.85	0.29	1.18	0.83	1.03	0.19	1.88	2.91	1.36	0.78	
Sigmoid	**4**	**64**	**C14**	2.19	0.3	1.33	0	0.47	0.34	0.33	0.61	1.44	0.78		
		128	**C15**	0.11	1.41	1.13	1.46	0.72	0.52	0.89	1.47	2.4	1.12		
		32	**C16**	2.19	2.16	0.02	0.99	1	1.56	0.27	1.92	3.03	1.46	0.94	
	6	**64**	**C17**	0.34	0.62	0.22	0.74	0.55	0.68	0.17	2.03	3.15	0.94		
		128	**C18**	0.14	1.64	1.89	1.57	0.68	0.75	0.21	1.72	2.85	1.27		
		32	**C19**	1.45	0.84	0.06	0.85	0.5	0.42	0.34	1.15	1.13	0.75	0.75	0.58
	2	**64**	**C20**	0.43	2.03	1.77	2.24	2.19	2.43	1.7	2.63	2.73	2.02		
		128	**C21**	1.66	0.51	1.81	1.57	2.1	2.05	2.53	1.8	1.93	1.77		
		32	**C22**	2.51	0.7	0	0.03	0.27	0.29	1.14	0.63	0.77	0.71	0.71	
Swish	**4**	**64**	**C23**	1.59	0.03	1.17	0.18	0.92	1.32	1.24	0.61	0.32	0.82		
		128	**C24**	0.48	2.75	1.43	1.96	1.34	1.39	1.35	2.39	2.79	1.77		
		32	**C25**	2.35	0.24	0.42	0.97	0.7	0.55	0.1	1.36	2.39	1.01	0.58	
	6	**64**	**C26**	0.96	1.71	0.94	0.04	0.67	0.46	1	0.39	1.04	0.8		
		128	**C27**	1.14	0.85	0.08	1.13	0.11	0.28	0.99	0.41	0.24	0.58		

Table 20. Error of hardness using linear.

ANN Architecture				Error of Hardness using Linear (%)										Best (Minimum)	
				H1	H2	H3	H4	H5	H6	H7	H8	H9	AVG	Config.	Activation
ReLU	2	32	C1	4.26	1.49	0.65	5.01	1.73	2.91	3.21	3.61	1.05	2.66	1.84	1.84
		64	C2	4.74	1.64	0.13	4.2	1	2.26	0.17	0.05	3.87	2.01		
		128	C3	2.47	0.01	1.54	4.47	1.43	1.83	1.41	1.67	1.72	1.84		
	4	32	C4	6.15	2.37	0.35	3.47	1.05	3.03	4.09	6.39	5.71	3.62	2.81	
		64	C5	5.21	1.71	1.04	2.78	0.88	1.79	2.17	4.86	4.84	2.81		
		128	C6	8	3.75	1.59	3.17	0.71	1.29	0.93	3.98	3.73	3.02		
	6	32	C7	3.09	1.2	0.97	4.19	2.65	4.72	5.69	8.46	8.47	4.38	2.65	
		64	C8	4.4	2.33	0.84	3.44	0.43	2	1.36	4.77	4.31	2.65		
		128	C9	5.14	3.28	2.61	1.94	0.96	2.36	1.46	3.88	5.4	3		
Sigmoid	2	32	C10	2.16	0.6	1.57	4.21	1.06	1.91	1.24	3.01	4.36	2.23	1.34	1.34
		64	C11	2.04	0.16	0.94	4.33	0.94	1.47	1.37	2.91	3.71	1.98		
		128	C12	1.08	0.12	0.61	3.95	0.91	1.27	0.54	1.04	2.56	1.34		
	4	32	C13	3.95	2.07	1.87	4.48	1.26	2.94	2.1	4.8	7.33	3.42	1.97	
		64	C14	1.4	0.68	1.49	3.92	0.83	1.6	0.93	2.6	5.2	2.07		
		128	C15	0.06	0.78	1.19	4.37	1.25	2.06	1.29	1.99	4.74	1.97		
	6	32	C16	5.33	2.59	1.61	5.25	1.25	1.82	0.22	4.11	6.93	3.23	2.19	
		64	C17	1.86	0.31	1.48	4.89	2.03	3.36	1.7	4.06	6.87	2.95		
		128	C18	1.72	0.68	1.15	3.97	1.08	2.19	1.06	2.49	5.36	2.19		
Swish	2	32	C19	0.84	1.08	1.71	5.59	2.06	1.58	1.77	2.32	4.8	2.42	1.2	1.2
		64	C20	0.29	1.45	1.92	4.19	0.71	1.14	0.59	1.88	0.55	1.41		
		128	C21	0.23	1.33	1.57	4.46	0.56	0.4	0.02	0.36	1.91	1.2		
	4	32	C22	1.98	0.73	1.98	5.12	1.79	1.78	0.16	1.72	1.03	1.81	1.81	
		64	C23	3.04	0.12	1.33	4.21	2.05	2.72	1.09	2.89	4.54	2.44		
		128	C24	1.63	0.56	1.24	5.03	2.02	3.05	2.89	4.64	4.88	2.88		
	6	32	C25	3.38	0.41	1.83	5.24	3	2.74	1.28	3.29	5.49	2.96	2.33	
		64	C26	2.98	0.32	1.39	4.58	1.63	1.29	1.67	2.5	4.62	2.33		
		128	C27	1.41	2.61	3.28	6.55	2.56	1.37	0.52	3.26	12.21	3.75		

Table 21. Error of hardness using logarithmic.

ANN Architecture				Error of Hardness using Logarithmic (%)										Best (Minimum)	
				H1	H2	H3	H4	H5	H6	H7	H8	H9	AVG	Config.	Activation
ReLU	2	32	C1	2.86	2.31	1.76	3.81	0.55	2.38	2.35	2.93	0.72	2.19	2.05	1.54
		64	C2	5.74	3.77	0.1	3.28	0.51	1.42	1.32	0.54	2.86	2.17		
		128	C3	5.24	3.36	1.91	3.26	0.86	0.77	0.35	0.44	2.25	2.05		
	4	32	C4	4.64	2.93	0.78	1.83	0.13	2.85	3.37	5.18	3.24	2.77	2.77	
		64	C5	9.41	5.85	1.75	1.44	1.11	1.37	1.83	3.66	2.78	3.24		
		128	C6	9.59	6.13	1.76	0.74	1.3	1.43	2.42	1.69	2.6	3.07		
	6	32	C7	8.5	5.2	0.29	1.88	0.05	2.05	1.41	4.45	3.94	3.08	1.54	
		64	C8	1.32	3.24	0.24	1.06	0.98	1.64	1.05	1.83	2.54	1.54		
		128	C9	8.23	7.13	3.24	0.23	3.36	1.11	0.54	2.78	5.32	3.55		
Sigmoid	2	32	C10	3.57	1.97	1.2	2.13	0.36	0.4	1.29	0.03	1.41	1.37	1.12	1.12
		64	C11	2.27	1.94	0.68	1.87	1.14	1.12	0.02	0.34	0.76	1.12		
		128	C12	2.35	1.86	1.61	1.97	1.76	1.04	1.06	1.59	3.09	1.81		
	4	32	C13	3.87	0.66	1.23	2.78	0.68	1.56	0.55	1.86	4.42	1.96	1.76	
		64	C14	2.45	2.14	1.61	3.12	0.3	2.56	1.23	1.19	3.96	2.06		
		128	C15	2.62	2.56	1.71	2.3	1.27	1.44	0.54	0.24	3.16	1.76		
	6	32	C16	5.49	3.21	0.31	2.88	0.27	2.01	0.2	1.08	3.97	2.16	1.63	
		64	C17	2.75	2.55	1.15	2.57	0.32	2.21	0.82	1.52	4.42	2.04		
		128	C18	1.05	1.81	0.52	1.84	0.87	2.03	0.69	1.47	4.37	1.63		
Swish	2	32	C19	2.44	1.69	1.49	3.35	0.73	1.58	0.19	0.73	1.29	1.5	1.44	1.37
		64	C20	3.09	2.96	0.42	2.8	1.04	1.34	0.44	0.78	0.1	1.44		
		128	C21	2.67	2.51	1.21	2.66	1.36	1.05	0.56	0.82	1.06	1.54		
	4	32	C22	4.03	1.31	1.47	3.48	0.33	1.03	0.41	0.65	1.02	1.52	1.37	
		64	C23	1.7	1.01	1.29	3	0.76	1.72	0.25	0.64	1.95	1.37		
		128	C24	5.96	5.77	2.96	1.41	1.34	1.66	2.73	3.78	3.95	3.28		
	6	32	C25	3.73	0.87	1.8	2.2	1.43	0.23	1.66	1	1.02	1.55	1.5	
		64	C26	5.08	2.6	1.08	3.62	0.8	0.18	0.29	0.26	2.19	1.79		
		128	C27	1.62	1.63	1.7	1.94	1.16	1.36	1.48	1.05	1.56	1.5		

Table 22. Error of hardness using exponential.

ANN Architecture				Error of Hardness using Exponential (%)										Best (Minimum)	
				H1	H2	H3	H4	H5	H6	H7	H8	H9	AVG	Config.	Activation
ReLU	2	32	C1	5.31	1.52	1.26	5.1	1.45	0.43	1	0.44	4.84	2.37	1.95	1.95
		64	C2	2.81	0.48	1.41	4.96	1.28	1.46	0.45	0.92	7.47	2.36		
		128	C3	4.45	0.09	1.62	4.39	1.14	1.19	0.6	0.8	3.23	1.95		
	4	32	C4	5.89	1.63	3.17	5.58	3.23	3.59	4.12	5.86	3.99	4.12	2.04	
		64	C5	12.04	4.86	0.71	3.51	1.01	2.68	2.03	3.7	2.39	3.66		
		128	C6	8.5	3.55	1.39	2.27	0.1	0.32	0.17	1.15	0.91	2.04		
	6	32	C7	12.35	4.37	0.61	2.43	1.72	2.07	2.9	5.51	5.01	4.11	2.85	
		64	C8	7.42	3.21	2.6	2.71	0.06	2.41	2.4	4.03	5.6	3.38		
		128	C9	6.35	2.25	1.49	2.89	0.06	1.59	1.68	3.7	5.68	2.85		
Sigmoid	2	32	C10	5.46	1.46	1.18	4.98	1.54	1.7	0.68	1.49	2.94	2.38	1.46	1.43
		64	C11	1.67	0.81	1.85	5.12	1.53	0.75	0.2	0.53	0.66	1.46		
		128	C12	2.84	0.5	1.19	4.09	0.44	0.19	1.12	2.3	2.08	1.64		
	4	32	C13	3.54	1.12	1.9	5.75	2.32	1.85	0.88	1.33	3.81	2.5	1.43	
		64	C14	3.19	0.36	1.88	5.18	1.92	1.75	1.17	0.51	3.21	2.13		
		128	C15	2.38	0.87	0.06	4.18	1.45	0.31	0.73	0.87	2.05	1.43		
	6	32	C16	6.88	1.54	0.62	4.53	1.42	0.78	1.3	1.9	4.76	2.64	1.69	
		64	C17	4.17	0.53	1.74	4.98	1.92	0.83	0.89	0.78	3.69	2.17		
		128	C18	2.28	0.67	0.79	4.9	2.34	1.04	0.3	0.34	2.58	1.69		
Swish	2	32	C19	3.61	0.5	1.49	4.13	1.15	1.46	0.16	1.14	0.49	1.57	1.57	1.36
		64	C20	1.93	0.57	1.83	6.04	2.02	0.88	0.86	0.24	3.66	2		
		128	C21	3.52	0.61	1.26	5.26	1.89	1.77	1.08	1.39	0.28	1.9		
	4	32	C22	3.87	0.2	1.15	5.73	2.78	2.25	1.32	2.24	0.19	2.19	1.65	
		64	C23	6.06	1.35	0.7	3.74	0.88	1.29	0.33	0.78	1.88	1.89		
		128	C24	5.29	1.12	1.04	4.03	0.85	0.73	0.43	0.99	0.42	1.65		
	6	32	C25	3.62	0.3	1.87	5.94	3.38	2.43	0.16	0.54	1.96	2.24	1.36	
		64	C26	3.76	1.11	0.61	4.86	2.54	1.25	0.25	0.36	1.22	1.77		
		128	C27	2.88	0.47	1.12	3.71	0.67	0.56	0.25	0.65	1.96	1.36		

Table 23. Error of hardness using polynomial.

ANN Architecture				Error of Hardness using Polynomial (%)										Best (Minimum)	
				H1	H2	H3	H4	H5	H6	H7	H8	H9	AVG	Config.	Activation
ReLU	2	32	C1	10.59	5.48	1.46	2.36	0.2	1.04	2.24	2.9	0.6	2.99	0.72	0.72
		64	C2	4.48	1.84	0.91	2.05	0.44	0.2	0.97	0.55	2.26	1.52		
		128	C3	1.01	0.33	0.41	1.27	1.16	0.36	0.44	0.79	0.72	0.72		
	4	32	C4	8.65	2.92	0.1	0.24	1.16	0.66	1.69	4.29	3.74	2.61	1.71	
		64	C5	6.25	2.11	1.07	1.97	0.47	0.03	0.14	2.17	1.2	1.71		
		128	C6	9.64	4.78	2.7	0.9	1.82	0.1	1.25	1.94	1.84	2.78		
	6	32	C7	1.82	0.33	1.14	2.53	0.68	1.85	2.45	5.84	6.21	2.54	2.54	
		64	C8	6.12	2.96	1.74	0.31	0.64	2.39	3.15	5.65	6.79	3.3		
		128	C9	7.79	4.3	2.78	0.34	0.12	0.32	0.06	4.1	4.67	2.72		
Sigmoid	2	32	C10	4.45	1.41	0.53	2.03	0.88	0.35	0.32	2.98	5.03	2	1.48	1.37
		64	C11	0.06	1.03	1.15	2.23	0.59	0.5	0.52	2.81	4.42	1.48		
		128	C12	0.54	1.57	1.4	2.36	0.06	0.92	0.13	1.96	4.34	1.48		
	4	32	C13	3.79	0.82	0.72	1.79	1.41	0.24	1.03	3.5	6.22	2.17	1.42	
		64	C14	1.65	1.26	0.15	1.67	0.88	0.56	0.12	1.88	4.59	1.42		
		128	C15	1.12	0.6	0.21	1.83	0.61	0.86	0.69	2.05	4.87	1.43		
	6	32	C16	3.97	1.55	1.24	2.12	0.15	1.16	0.77	4.1	6.91	2.44	1.37	
		64	C17	2.06	0.04	0.01	0.71	1.45	0.17	0	2.52	5.37	1.37		
		128	C18	0.72	0.47	0.51	1.59	0.03	0.91	0.22	2.79	5.65	1.43		
Swish	2	32	C19	1.57	0.18	0.95	2.1	1.14	0.33	1.07	0.87	0.16	0.93	0.93	0.93
		64	C20	1.55	0.14	1.02	1.29	1.6	0.72	1.5	0.55	0	0.93		
		128	C21	2.02	3.11	3.49	3.25	0.1	0.84	0.79	0.94	0.04	1.62		
	4	32	C22	0.7	1.3	1.62	1.79	0.43	0.05	0.53	2.53	4.04	1.44	1.16	
		64	C23	1.26	0.54	1.29	1.89	0.63	0.08	1.38	1.15	2.26	1.16		
		128	C24	1.04	1.54	2.17	2.95	0.18	0.39	0.56	1.36	0.77	1.22		
	6	32	C25	2.11	0.45	0.59	2.26	0.35	0.02	0.18	3.04	4.19	1.47	1.47	
		64	C26	0.46	1.16	1.45	2.69	0.11	0.01	0.21	2.32	4.38	1.42		
		128	C27	1.48	0.7	1.28	0.94	1.72	0.35	0.2	1.92	4.64	1.47		